APACHE

Analysis of climate feedback PArameter Changes from Heat Evolution

Algorithm Theoretical Basis Document

	Name	Organisation	Date	Visa
Written by:	Michaël Ablain Camille Szczypta Robin Fraudeau Victor Rousseau Zacharie Barrou Dumont	Magellium	23/02/2025	
	Benoit Meyssignac	LEGOS		
Checked by:	Michaël Ablain	Magellium	23/02/2025	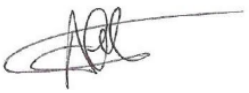
Approved by:	Joël Dorandeu	Magellium	23/02/2025	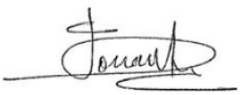

Document reference:	GIECCO-DT-135-MAG_ATBD_climate_sensitivity
Edition.Revision:	1.0
Date Issued:	23/02/2025
Data Set Version:	v1-0

Document evolution sheet

Ed.	Rev.	Date	Purpose evolution	Comments
1	0	23/02/2025	Creation of document	

Contents

List of tables

List of figures

1. Introduction

1.1. Executive summary

This document is the Algorithm Theoretical Basis Document (ATBD) of the processing chain calculating the APACHE climate sensitivity products (sensitivity and feedback parameters). This ATBD is dedicated to the description and justification of the algorithms used in the generation of the products.

1.3. Document structure

In addition to this introduction, the document is organised as follows:

- Section 2 explains the physical principle
- Section 3 presents the input data of the processing chain.
- Section 4 provides a detailed description and justification of every step in the computation.
- Section 5 provides a detailed description and justification of the uncertainty propagation methodology until the final product.

1.4. Applicable documents

Id.	Ref.	Description
AD1	GIECCO-DT-136-MAG_PUM_climate_sensitivity	Product user manual (PUM)

Table 1: List of applicable documents

1.6. Bibliography

- Budyko, M. I.: The effect of solar radiation variations on the climate of the Earth, Tellus, 21, 611–619, https://doi.org/10.3402/tellusa.v21i5.10109, 1969.
- Charney, J. G., Arakawa, A., Baker, D. J., Bolin, B., Dickinson, R. E., Goody, R. M., Leith, C. E., Stommel, H. M., and Wunsch, C. I.: Carbon dioxide and climate: a scientific assessment, National Academy of Sciences, Washington, DC, 1979.
- Cheng, L., Trenberth, K. E., Fasullo, J., Boyer, T., Abraham, J., and Zhu, J.: Improved estimates of ocean heat content from 1960 to 2015, Sci. Adv., 3, e1601545, https://doi.org/10.1126/sciadv.1601545, 2017.

- Cheng, L., Trenberth, K. E., Gruber, N., Abraham, J. P., Fasullo, J. T., Li, G., Mann, M. E., Zhao, X., and Zhu, J.: Improved Estimates of Changes in Upper Ocean Salinity and the Hydrological Cycle, J. Clim., 33, 10357–10381, https://doi.org/10.1175/JCLI-D-20-0366.1, 2020.
- Cowtan, K. and Way, R. G.: Coverage bias in the HadCRUT4 temperature series and its impact on recent temperature trends, Q. J. R. Meteorol. Soc., 140, 1935–1944, https://doi.org/10.1002/qj.2297, 2014.
- Forster, P. M., Smith, C. J., Walsh, T., Lamb, W. F., Lamboll, R., Hauser, M., Ribes, A., Rosen, D., Gillett, N., Palmer, M. D., Rogelj, J., von Schuckmann, K., Seneviratne, S. I., Trewin, B., Zhang, X., Allen, M., Andrew, R., Birt, A., Borger, A., Boyer, T., Broersma, J. A., Cheng, L., Dentener, F., Friedlingstein, P., Gutiérrez, J. M., Gütschow, J., Hall, B., Ishii, M., Jenkins, S., Lan, X., Lee, J.-Y., Morice, C., Kadow, C., Kennedy, J., Killick, R., Minx, J. C., Naik, V., Peters, G. P., Pirani, A., Pongratz, J., Schleussner, C.-F., Szopa, S., Thorne, P., Rohde, R., Rojas Corradi, M., Schumacher, D., Vose, R., Zickfeld, K., Masson-Delmotte, V., and Zhai, P.: Indicators of Global Climate Change 2022: annual update of large-scale indicators of the state of the climate system and human influence, Earth Syst. Sci. Data, 15, 2295–2327, https://doi.org/10.5194/essd-15-2295-2023, 2023.
- Frederikse, T., Landerer, F., Caron, L., Adhikari, S., Parkes, D., Humphrey, V. W., Dangendorf, S., Hogarth, P., Zanna, L., Cheng, L., and Wu, Y.-H.: The causes of sea-level rise since 1900, Nature, 584, 393–397, https://doi.org/10.1038/s41586-020-2591-3, 2020.
- Good, S. A., Martin, M. J., and Rayner, N. A.: EN4: Quality controlled ocean temperature and salinity profiles and monthly objective analyses with uncertainty estimates, J. Geophys. Res. Oceans, 118, 6704–6716, https://doi.org/10.1002/2013JC009067, 2013.
- Ishii, M., Fukuda, Y., Hirahara, S., Yasui, S., Suzuki, T., and Sato, K.: Accuracy of Global Upper Ocean Heat Content Estimation Expected from Present Observational Data Sets, Sola, 13, 163–167, https://doi.org/10.2151/sola.2017-030, 2017.
- Levitus, S., Antonov, J. I., Boyer, T. P., Baranova, O. K., Garcia, H. E., Locarnini, R. A., Mishonov, A. V., Reagan, J. R., Seidov, D., Yarosh, E. S., and Zweng, M. M.: World ocean heat content and thermosteric sea level change (0–2000 m), 1955–2010, Geophys. Res. Lett., 39, https://doi.org/10.1029/2012GL051106, 2012.
- Meyssignac, B., Boyer, T., Zhao, Z., Hakuba, M. Z., Landerer, F. W., Stammer, D., Köhl, A., Kato, S., L'Ecuyer, T., Ablain, M., Abraham, J. P., Blazquez, A., Cazenave, A., Church, J. A., Cowley, R., Cheng, L., Domingues, C. M., Giglio, D., Gouretski, V., Ishii, M., Johnson, G. C., Killick, R. E., Legler, D., Llovel, W., Lyman, J., Palmer, M. D., Piotrowicz, S., Purkey, S. G., Roemmich, D., Roca, R., Savita, A., Schuckmann, K. von, Speich, S., Stephens, G., Wang, G., Wijffels, S. E., and Zilberman, N.: Measuring Global Ocean Heat Content to Estimate the Earth Energy Imbalance, Front. Mar. Sci., 6, https://doi.org/10.3389/fmars.2019.00432, 2019.
- Meyssignac, B., Chenal, J., Loeb, N., Guillaume-Castel, R., and Ribes, A.: Time-variations of the climate feedback parameter λ are associated with the Pacific Decadal Oscillation, Commun. Earth Environ., 4, 1–10, https://doi.org/10.1038/s43247-023-00887-2, 2023.
- Morice, C. P., Kennedy, J. J., Rayner, N. A., Winn, J. P., Hogan, E., Killick, R. E., Dunn, R. J. H., Osborn, T. J., Jones, P. D., and Simpson, I. R.: An Updated Assessment of Near-Surface Temperature Change From 1850: The HadCRUT5 Data Set, J. Geophys. Res. Atmospheres, 126, e2019JD032361, https://doi.org/10.1029/2019JD032361, 2021.

- Pincus, R., Forster, P. M., and Stevens, B.: The Radiative Forcing Model Intercomparison Project (RFMIP): experimental protocol for CMIP6, Geosci. Model Dev., 9, 3447–3460, https://doi.org/10.5194/gmd-9-3447-2016, 2016.
- Richardson, M., Cowtan, K., Hawkins, E., and Stolpe, M. B.: Reconciled climate response estimates from climate models and the energy budget of Earth, Nat. Clim. Change, 6, 931–935, https://doi.org/10.1038/nclimate3066, 2016.
- von Schuckmann, K., Minière, A., Gues, F., Cuesta-Valero, F. J., Kirchengast, G., Adusumilli, S., Straneo, F., Allan, R., Barker, P. M., Beltrami, H., Boyer, T., Cheng, L., Church, J., Desbruyeres, D., Dolman, H., Domingues, C., García-García, A., Giglio, D., Gilson, J., Gorfer, M., Haimberger, L., Hendricks, S., Hosoda, S., Johnson, G. C., Killick, R., King, B. A., Kolodziejczyk, N., Korosov, A., Krinner, G., Kuusela, M., Langer, M., Lavergne, T., Li, Y., Lyman, J., Marzeion, B., Mayer, M., MacDougall, A., Lawrence, I., McDougall, T., Monselesan, D. P., Nitzbon, J., Otosaka, I., Peng, J., Purkey, S., Roemmich, D., Sato, K., Sato, K., Savita, A., Schweiger, A., Shepherd, A., Seneviratne, S. I., Simons, L., Slater, D. A., Slater, T., Smith, N., Steiner, A. K., Suga, T., Szekely, T., Thiery, W., Timmermanns, M.-L., Vanderkelen, I., Wijffels, S. E., Wu, T., and Zemp, M.: Heat stored in the Earth system 1960-2020: Where does the energy go?, 2022.
- Smith, C., Hall, B., Dentener, F., Ahn, J., Collins, W., Jones, C., Meinshausen, M., Dlugokencky, E., Keeling, R., Krummel, P., Mühle, J., Nicholls, Z., and Simpson, I.: IPCC Working Group 1 (WG1) Sixth Assessment Report (AR6) Annex III Extended Data (v1.0), https://doi.org/10.5281/ZENODO.5705391, 2021.

1.7. Terminology

Abbreviation/acronym	Description
ATBD	Algorithm theoretical basis document
BAR	Barystatic sea level
CS	Climate Sensitivity
DOI	Digital Object Identifier
ECS	Equilibrium climate sensitivity
EEI	Earth Energy Imbalance
ERF	Effective radiative forcing
EWH	Equivalent water height
GM	Global mean
GOHC	Global ocean heat content
GOHU	Global ocean heat uptake
GMSL	Global mean sea level
GMST	Global mean surface temperature
GMSSL	Global mean steric sea level
IPCC	Intergovernmental Panel on Climate Change
NetCDF	Network common data form

OHC	Ocean heat content
PUM	Product user manual
SL	Sea level
SLB	Sea level budget
SST	Sea Surface Temperature
TOA	Top-of-Atmosphere

Table 2: List of abbreviations and acronyms

2. Physical principle

The aim of this project is to provide an estimate of the climate feedback parameter λ over time. In the framework of climate change, relating to the evolution of greenhouse gases, the concept of Climate Sensitivity (CS) emerges for a quantitative measurement of the amount of warning (in Kelvin) associated with the increase of atmospheric CO_2 concentration. High climate sensitivity means that small changes in greenhouse gas concentrations can lead to significant variations in the global climate, while lower sensitivity implies more limited changes. Understanding climate sensitivity is therefore crucial for studying current and future climate changes. Equilibrium Climate Sensitivity (ECS) represents the Earth's global average surface temperature reached after an instantaneous doubling of atmospheric carbon dioxide concentration compared to pre-industrial level. Jonathan Chenal's Phd work focused on estimating this quantity, notably through a comprehensive literature review. There are two ways to determine ECS: either by simulating it from climate numerical models (which can simulate an equilibrium state) or by estimating it from climate system observations. Today, ECS remains poorly understood, and since the Charney et al., (1979) report to the fifth IPCC report in 2014, its range of values extends from 1.5 to 4.5°C. The lower bound is particularly due to marked biases in instrumental measures, while the upper bound is due to estimation errors related to climate models. This wide range of values is due to the fact that ECS varies over time, particularly in relation to the radiative effect of spatial structures of surface warning, which can be induced by internal climate variability or historical variations in atmospheric composition. In our work and because ECS can not be directly measured, we focus on estimating ECS from time series of observations. In this context, it is first necessary to define the climate feedback parameter, called λ, which describes the magnitude of the Earth's radiative response to a change in global average 2-metre surface temperature (T). More specifically, it quantifies how the heat fluxes (radiative forcing) between the Earth and space are modified in response to a variation in surface temperature. Thus, climate sensitivity is directly related to this λ parameter, as a less negative λ value implies a weaker radiative response to a given change in surface temperature, leading to greater climate sensitivity.

2.1. The climate feedback parameter λ

The radiative forcing (F), largely driven by CO_2, causes other elements of the climate system to react by damping or amplifying the warning. This response is referred to as feedback and is quantified by the climate feedback parameter λ, also defined as the parameter which

determines the magnitude of the Earth radiative response to a given change in global mean surface temperature (GMST). If λ plays a central role in the Earth's climatic response to an increase in CO2 concentration, it is currently poorly constrained and thus subject to significant uncertainties. The ECS, which depends on λ, is therefore very sensitive to the uncertainties in the λ estimates. Reducing the uncertainty in the estimate of ECS thus necessarily involves better estimating the λ parameter, particularly by successfully constraining it more effectively. The difficulty in constraining λ lies in the fact that it can not be directly measured and must therefore be estimated through various methods based on the global energy balance approach (Budyko, 1969), which is defined as:

$$\Delta N = \Delta F + \lambda \Delta T \qquad \text{Equation 11}$$

N represents the Planetary Heat Uptake, which represents the Earth's Energy Imbalance (EEI), and is broken down into a term F, representing the radiative forcing and a term λT, representing the Earth's radiative response, with λ being the climate feedback parameter and T the surface temperature of the Earth at 2 metres. In the current transient regime that characterises contemporary climate change, solving the energy balance equation (Equation 1) allows for an estimation of λ. This estimation can be done in several ways but in our study, we focus on the method based on a linear regression of the energy budget. A major problem with all these observational methods (and also with the used regression approach) is that they provide estimates of the λ parameter during the historical period, which are potentially different from the equilibrium climate feedback parameter λeq, which is the one we are aiming to calculate. Over a defined time period, the historical λ parameter is related to the radiative forcing change (ΔF), the global mean temperature variation (ΔT) and the evolution of planetary heat uptake (ΔN), by the global energy budget also deduced from the Equation 2 and described by the following equation:

$$\lambda = \frac{\Delta N - \Delta F}{\Delta T} \qquad \text{Equation 2}$$

We use a differential form of the energy budget and regress ΔN - ΔF on ΔT for time windows of more than 25 years starting from 1957. We use this approach rather than others because regressions are a better estimator of the λ parameter, they make full use of available data and they rely on recent instrumental data without depending on a late 19th century reference state that is still largely unknown. The radiative forcing, temperature anomaly and planetary heat uptake data required to calculate the regressions are described in section 3 "Input data".

2.2. The equilibrium climate sensitivity (ECS)

The ECS is the equilibrium surface temperature response to a doubling of atmospheric CO2 concentrations. It is inversely related to the climate feedback parameter λ by the global energy budget of the climate system at equilibrium:

$$ECS = \frac{\Delta F2x}{\lambda eq} \qquad \text{Equation 3}$$

Where ΔF_{2x} is the forcing anomaly due to doubling atmospheric CO_2 concentrations. Because of the inverse relation (Equation 3), the uncertainty in the climate feedback parameter is increased when propagated in ECS error budget and it becomes the dominant source of ECS uncertainty.

3. Input data

3.1. Overview

The following section describes the different datasets used to estimate the λ parameter over long time periods. They include time-varying data such as the Global Mean Surface Temperature (GMST, or T for temperature), the radiative forcing (F) and the planetary heat uptake (EEI or N). Knowledge of the variation in these three variables over a given period compared with a state considered to be initial, enables calculation of the λ parameter for the relevant window. To determine the temporal evolution of planetary heat uptake, the energy absorbed by each of the 4 terrestrial reservoirs needs to be considered and then summed. Energy absorption as heat is higher in the ocean reservoir than others and its quantification is derived from Ocean Heat Uptake (OHU) timeseries, obtained by different approaches which are detailed in the following section related to the planetary heat uptake variable. The associated variables used to estimate OHU are also described in the same section. To produce the different time series of variables, the period 1850 to 1900 is considered as the reference state (the period defined by the IPCC).0

3.2. Radiative forcing

For the radiative forcing F, we use the ensemble of effective radiative forcing (ERF) from the IPCC AR6 (Smith et al., 2021). The IPCC AR6 ERF is computed from two prescribed SST and sea-ice experiments after removing the top of the atmosphere energy budget change associated with the land surface temperature response. It also includes the aerosol and the non-aerosol cloud adjustments. Note however that the IPCC ERF only accounts for the direct radiative effect of the land surface temperature response and not the indirect effect on water vapour and tropospheric temperature (Meyssignac et al., 2023), but it can be noted that the latter effect is small, of the order of a tenth of W.m-2 (Forster et al., 2023).

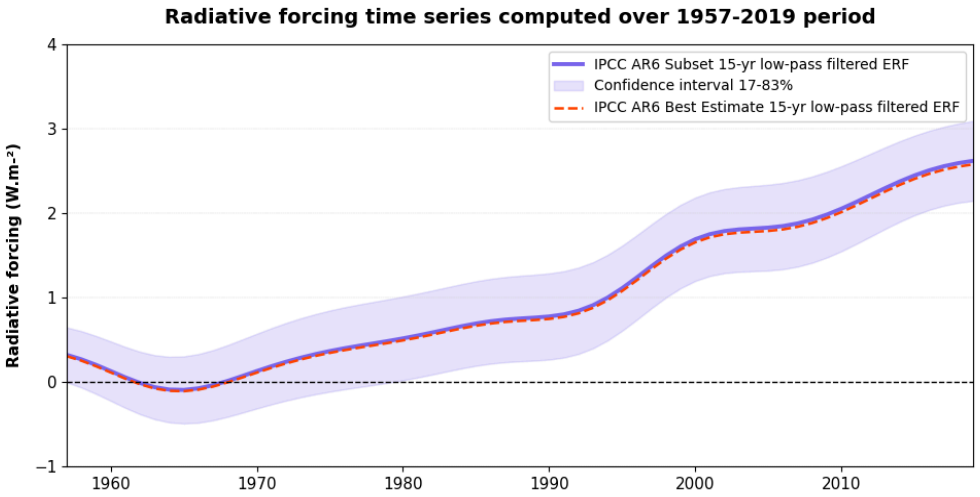

Figure 1. IPCC AR6 ERF time series computed from the ensemble of randomly selected 500 solutions (in purple) and the best estimate solution (in orange) over the 1957-2019 period, by considering the reference state of 1850-1900.

As a product, we use the ensemble of 100.000 time series of the IPCC AR6 ERF, from which we randomly select N solutions. We initially selected 500 solutions as was done in previous Meyssignac et al., (2023) study, and then we also conducted the experiment by increasing this number of members to subsequently observe the impact this could have on the λ estimates. The N selected members are initially filtered using a simple 15-year filter. The average of our set of initially 500 filtered time series is then used as the input to our processing chain. The IPCC also provides a best-estimate ERF time series, which we have retrieved to compare with our previously calculated ensemble mean, then used as an input to our λ parameter processing chain. The ensemble of 100.000 solutions and the best estimate timeserie have been downloaded from here. Figure 1 illustrates these points. Averages and uncertainties are shown for the period since 1957 and up to 2019 (data availability). The series obtained from (1) the random subset of 500 members and (2) the "best estimate" solution are very close, if not practically identical. The random subset of 500 members reproduces the mean and variability of the 100.000 solutions of the initial ensemble (not shown).

3.3. Global Mean Surface Temperature

For the GMST time series, the HadCRUT4 v2 dataset (Cowtan and Way, 2014) , covering the 1850-2021 time period, is used as input of the first version of the λ parameter processing chain. Following the recommendation (Richardson et al., 2016), a scale factor of 1.09 is applied to this dataset, which is a blend of two (1) land surface temperature and (2) sea surface temperature (SST) datasets, to correct for the bias induced by the SST part of the combined dataset. Because the HadCRUT4 product is depreciated, the new HadCRUT5 (Morice et al., 2021), available from 1850 to present and based on new versions of land surface temperature and SST products, is then used as input to describe the GMST temporal evolution. Whereas the HadCRUT4 product was based on a set of 100 solutions, the new HadCRUT5 product is enhanced by a statistical method enabling the spatial coverage of data availability to be extended, which in practice doubles the number of ensemble solutions, which for HadCRUT5

is now composed of 200 members. The scale factor of 1.09 is used as well to convert the part of SST in 2-metre air temperature (T2m), in the HadCRUT5 ensemble dataset. For both HadCRUT datasets, the global mean of the ensemble is computed from the ensemble and then considered. The HadCRUT4 v2 product has been downloaded here and the HadCRUT5 here.

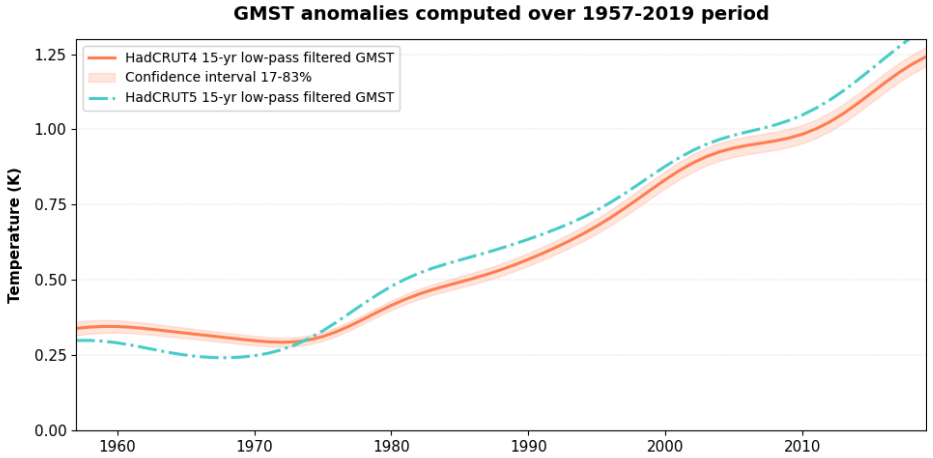

Figure 2 GMST anomalies computed over the 1957-2024 period (compared to the 1850-1956 pas period) for the HadCRUT4 et the HadCRUT5 products.

Figure 2 shows the 2 time series obtained from each of the 2 products over the period 1957 to 2024. The temperature anomalies are calculated on the basis of past temperatures over the GIEC reference period 1850-1900. This global mean temperature value obtained over the past period is then subtracted from the temperature time series over the 1957-2024 period to obtain temperature anomalies (see section 4.5.2).

3.4. Planetary heat uptake

To quantify the planetary heat uptake, the heat stored in each of the four climate system reservoirs, i.e (1) in the cryosphere, (2) in the atmosphere, (3) in land and (4) in the ocean, may be summed. Regarding the heat stored in land, cryosphere and atmosphere, it represents approximately only 7% of the total planetary heat uptake. The greatest proportion of heat (~93%) is therefore absorbed by the oceans. To estimate the heat uptake at the planetary scale, the heat uptake of each reservoir needs to be quantified. This calculation is based on a 2-stage process: firstly, the heat absorbed and contained in the 3 components, i.e. the cryosphere, the continental surfaces and the atmosphere, and secondly, a study of changes in the ocean heat content. Once the different components of heat uptake have been precisely quantified, a simple summation of the time series is then performed to determine the whole time series of planetary heat uptake since 1957. This section describes the components, and Figure 3 shows the computed time series over the 1957-2020 period, depending on the availability of data (see section 4.4.1.2.5.).

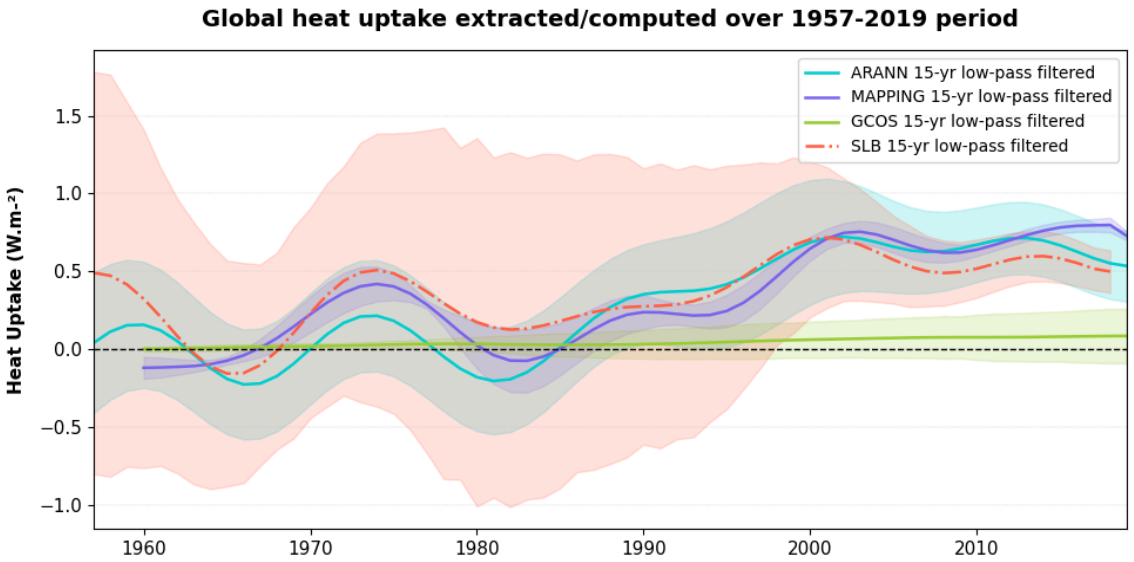

Figure 3. Heat uptake computed over the 1957-2020 period for the grouped (1) cryosphère, atmosphere and continental reservoirs (in green) and for the (2) ocean reservoir. Several datasets are used to describe the ocean heat uptake: the ARANN product (in turquoise), the mapping solution based on in situ datasets (in purple) and a dataset computed from the sea level budget (in orange)

3.4.1 Ocean heat uptake

The Ocean Heat Uptake (OHU) is essential for determining N and then deducing the λ parameter. To define a series of OHU, a set of three datasets was considered/calculated, and the time series used for the continuation of the study is derived from the average of these three datasets, to which a time series of uncertainties based on the dispersion of the ensemble of three solutions as well as the inherent uncertainty of each dataset is then associated.

- The first series, called the ARANN solution, comes from the ARANN OHU time series, which can be downloaded here. This series is obtained from various in situ temperature data products from which an OHC is deduced, and from an artificial intelligence approach using neural networks. The file containing the ARANN OHU also provides information on the uncertainty associated with this data time series.
- The second dataset, called the MAPPING solution, is obtained from five in situ Ocean Heat Content (OHC) products, i.e. two EN4 datasets (Good et al., 2013), the IMRI-JMA ISHII dataset (Ishii et al., 2017), the IAP (Cheng et al., 2017, 2020) dataset and the World ocean atlas dataset (Levitus et al., 2012).
- The third dataset, called the thermosteric solution (referred to as Sea Level Budget SLB), is obtained using the thermosteric component of sea level (Frederikse et al., 2020), produced from data measured by tide gauges and satellite altimetry and gravimetry products to which the sea level budget equations have been applied (Meyssignac et al., 2019). The data are available here.

Three OHU datasets are thus produced (the ARANN, the MAPPING and the SLB solutions), to make the best use of available observations, which also helps to reduce the limitations specific to each product and thereby limit the uncertainty, particularly related to the lack of observations in the deep ocean.

3.4.2 Cryosphere, continental and atmosphere heat uptake

We use the most recent estimate of this heat described in (von Schuckmann et al., 2022). The file containing the temporal evolution of heat content from the different reservoirs can be downloaded here. Heat content datasets are available in a netCDF file and are independently stored for each climate system reservoir. Data are given as global mean in the form of time series.

3.4. Volcanic eruptions

The time series of F, N and T are affected by three major volcanic eruptions between 1957 and 2017: Agung (1963), El Chichon (1982) and Pinatubo (1991). In order to evaluate and correct their effect we use climate model simulations of F_{sim}, N_{sim}, and T_{sim} of the historical period following the methodology of Meyssignac et al., (2023). Climate model simulations of the historical period do not have the same realization of the internal variability as the real-world climate so they cannot be used directly to evaluate the effect of volcanic eruptions. From each model we use large ensembles of historical simulations to remove the internal variability and isolate the forced response of climate:

For each realisation, we calculate the impact of the volcanic eruption $N_{eruption}$ and $T_{eruption}$ during the years following an eruption by subtracting the N_{sim} and T_{sim} value of the year preceding the eruption. In each large ensemble, we take the median across realizations in $N_{eruption}$ and $T_{eruption}$ during the 3 years following the eruptions of Agung, El Chichon and Pinatubo. We then calculate the multi-model mean time series of $N_{eruption}$ and $T_{eruption}$ and subtract them from the historical time series N and T to correct them for volcanic eruptions (see section 4.5.2.2).

Each realisation consists of 4 time series, one of T_{sim}, one of rlut (TOA Outgoing Longwave Radiation), one of rsdt (TOA Incident Shortwave Radiation), and one of rsut (TOA Outgoing Shortwave Radiation). N_{sim} is calculated by subtracting rlut and rsut from rsdt. We used all the available realisations from the models CanESM5 (42 realisations), GISS-E2-1-G (40 realisations), and MIROC6 (10 realisations).

To correct F we use the simulation of the historical period forced with natural forcing only and forced at the surface boundary with the SST of the control simulation (the so called piclim-histnat simulation from the Radiative Forcing Model Intercomparison Project phase 6 (Pincus et al., 2016)). In this simulation the radiative response is null because the SST is kept at the level of the control simulation so the TOA radiative imbalance N_{sim} gives an estimate of the forcing F_{sim} (which is here the natural forcing). We isolate the change of forcing $F_{eruption}$

during the 3 years following the eruptions of Agung, El Chichon and Pinatubo with the same method used for $N_{eruption}$ and $T_{eruption}$ and use this estimate to correct the historical time series F (see section 4.5.2.2).

4. Climate feedback parameter processing chain

4.1. Overview

The algorithms applied in the Climate Sensitivity processing chain are described in the following subsections in agreement with the summary Figure 4:

- The preprocessing of global mean surface temperature (GMST)
- The preprocessing of radiative forcing (ERF)
- The preprocessing of planetary heat uptake (EEI)
- The calculation of λ parameter by regression

4.2. input data

The processing chain, which allows to compute the λ parameter over time, is configured to use the following input data, described in section 3 and post-processed in section 4.5.2. Additionally, this process enables modification of the datasets considered through a YAML configuration file.

- One time series of EEI (N) completed by its uncertainty envelope over the 1957-2019 period.
- One time series of GMST (T) over the 1850-2024 period.
- 6000 time series of radiative forcing (F) over the 1750-2019 period.

4.3. Output data

The main product of this project contains the climate feedback parameter λ produced by regression of the post-processing data for all time windows longer than 25 years from 1957 to 2019. That is, for a window of 25 years, an annual vector ranging from 1970 to 2005 (central date of the window). λ uncertainties are also generated for the 25 year window.

The format of the product is described in detail in the product user manual (PUM). An additional product, called the extended product, is available, and contains the time series of

the post-processed input data used in the regression.

4.4. Retrieval methodology and uncertainty calculation & propagation

4.4.1. Post-processing of inputs data

4.4.1.1. Description

The diagram in Figure 4 illustrates the various stages of the post-processing chain for input data. Initially, radiative forcing (section 3.2), surface temperature (3.3) and data that subsequently allow the calculation of planetary heat uptake (section 3.4) are collected via different file formats (netCDF for some, ASCII for others, HDF5, etc.). All of these are available at different time steps depending on the datasets, ranging from monthly to annual time steps over periods from 1850 to the present for the longest datasets and at a minimum over the 1960-2019 period (boundaries determined by the most limiting time series). For the planetary heat uptake component, we use three time series for heat content in the (1) cryosphere, (2) atmosphere and (3) land (section 3.4.2). To calculate the ocean heat uptake component, three types of data are used (section 3.4.1): (1) a time series of ocean heat uptake (OHU) based on several in situ data and artificial intelligence methods, (2) time series of ocean heat content (OHC) based on several in situ data products, and (3) an ensemble of time series for the thermosteric sea level (TSL) component based on satellite product for recent periods and tide gauge measurements for older periods.

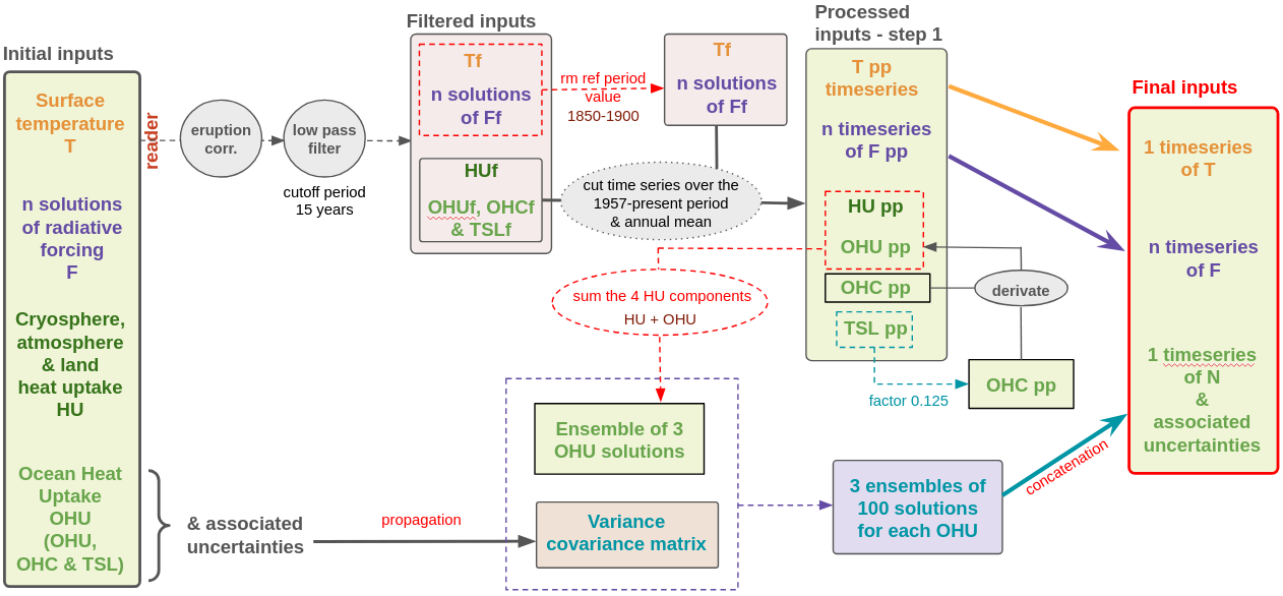

Figure 4. Input post-processing chain. It transforms a time series of surface temperature and radiative forcing into a time series of anomalies relative to a reference period. It also transforms a time series of heat uptakes of the oceans, cryosphere, atmosphere and land) into a time series of Earth energy imbalance plus its incertitudes.

4.4.1.2. Mathematical statement

4.4.1.2.1. Volcanic eruption correction

The first step involves reading the different files and retrieving the raw time series. F and T are directly corrected for volcanic eruptions by subtracting from them $F_{eruption}$ and $T_{eruption}$ (see section 3.4). The correction for N is applied after it is calculated in section 4.5.2.2.5.

4.4.1.2.2. Temporal filtering

The n time series of F and the time series of T are then temporally filtered using a 15-year low-pass filter.

4.4.1.2.3. Anomalies calculation based on a reference period

The filtered time series for temperature and radiative forcing can subsequently be recalculated as anomalies relative to a reference period or not; the key point is that they are processed consistently to avoid biasing the estimate of λ later on. In our case, we chose to recalculate these series (one series for temperature and n series for radiative forcing, representing a set of n forcing solutions) using the period from 1850-1900 as the reference period (the same considered by the IPCC).

4.4.1.2.4. Period selection

The next step involves generating annual series from those with finer time steps and truncating the series to the period from 1957 to 2019. At this stage of the process, the temperature and radiative forcing series are saved in netCDF files and considered ready for subsequent use in regression computation. The remaining post-processing of the input data pertains to the planetary heat uptake term, which is also used for the estimation of the λ parameter.

4.4.1.2.5. Post-processing chain to compute EEI time series

The time series of heat content for the atmosphere, land, and cryosphere reservoirs are derived to obtain heat uptake time series, which is the variable of interest for regression calculations. The different datasets of the ocean reservoir are also processed into OHU time series:

- The ARANN dataset already consists of a OHU time series with its associated uncertainty.
- The five OHC time series of the MAPPING dataset are first derived to generate five OHU time series, which are then averaged to create a single in situ OHU time series.
- The SLB dataset is composed of an ensemble of 5000 solutions. Each solution is first converted from the thermosteric component of sea level into OHC using an expansion coefficient of 0.125 (Levitus et al., 2012), then transformed into a OHC series, and derived into a OHU series. The SLB ensemble is then averaged into a single OHU series.

For the MAPPING and SLB datasets, the OHU uncertainties are obtained through the standard deviation of their ensembles after derivation.

Once the heat absorption component in the three non-ocean reservoirs is known and the calculation of the three Ocean Heat Uptake (OHU) values, each associated with their uncertainty envelopes, is completed, three time series of Earth's Energy Imbalance (EEI) are generated by adding the OHU series to the sum of the heat absorption in the three other GCOS reservoirs. From these three EEI series and the knowledge of the sigma series associated with each, three variance-covariance matrices are generated by filling the diagonal elements with the variances (i.e., the series of squared standard deviations) and the off-diagonal elements with zeros, assuming that all elements are strictly independent. Each matrix thus represents the variability of each EEI time series.

From these matrices, 100 random time series are generated, all contained within the uncertainty envelope of the considered EEI dataset. The three sets of 100 time series are then concatenated to obtain an EEI ensemble of 300 members. The EEI time series is therefore equal to the ensemble mean, and the associated sigma time series is calculated from this ensemble of 300 solutions, over the 1957-2019 time period.

The Figure 5 below shows the EEI series obtained using the previously described method and its uncertainty envelope.

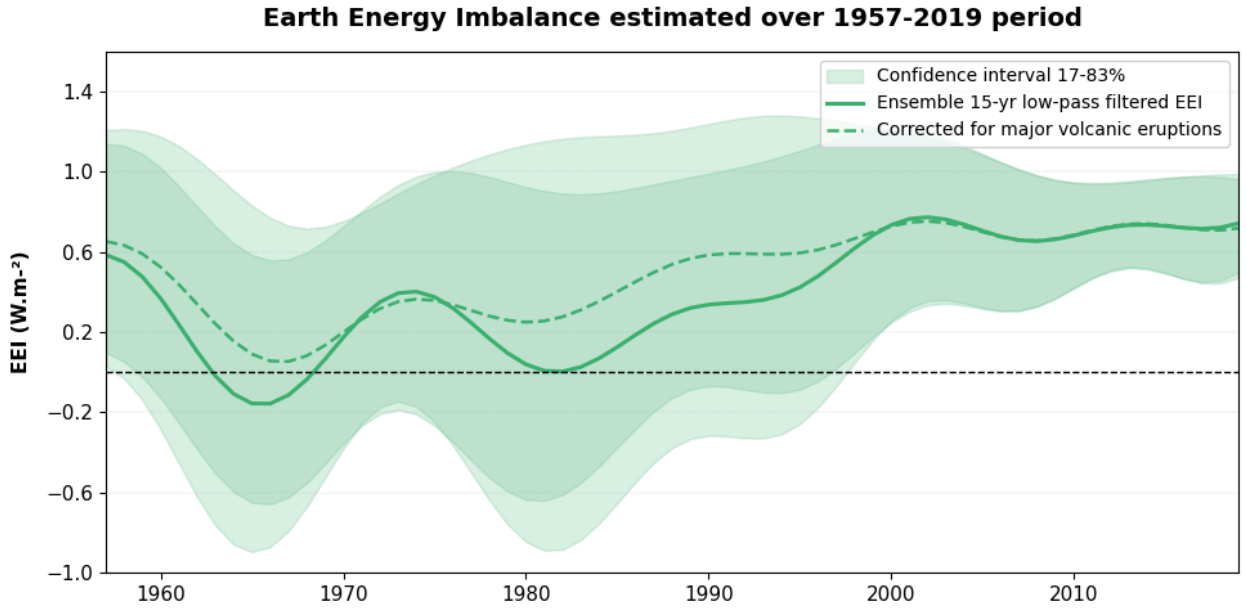

Figure 5. 300 solutions of EEI displayed as the mean with a confidence interval (17-83%).

4.4.2. Computation of λ parameter by regression

4.4.2.1. Description

The diagram in Figure 6 illustrates the generation of λ time series from the post-processed inputs: one time series of the temperature anomaly T, n time series of radiative forcing anomaly solutions F, and one time series of EEI with its uncertainties. Each time series covers the same 1957-2019 period and the same time step.

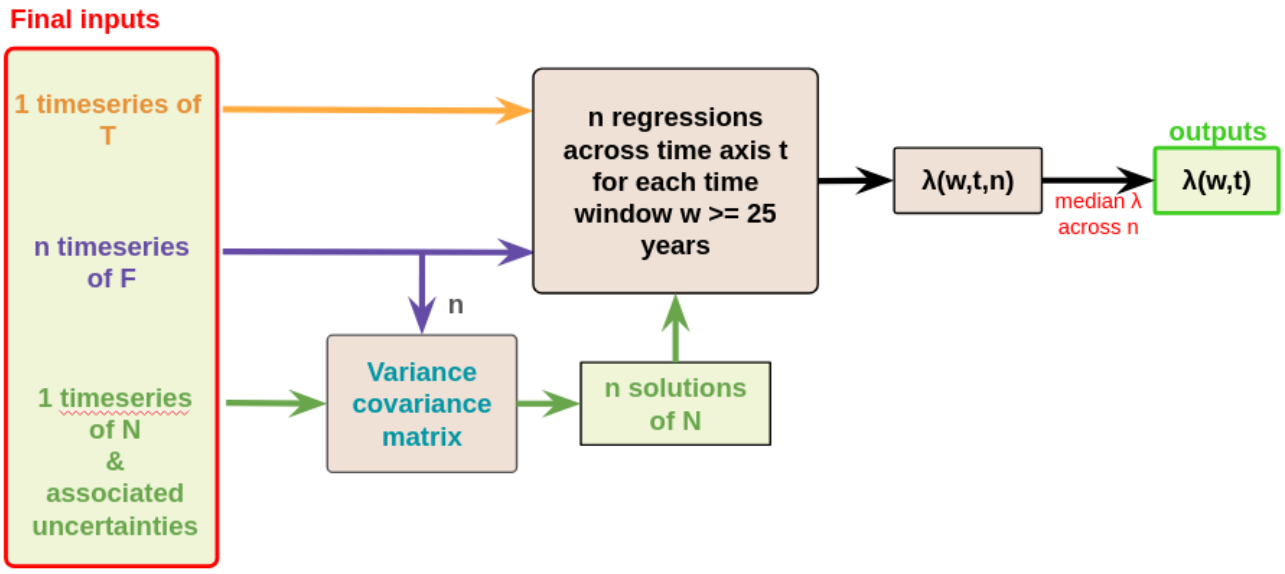

Figure 6. Climate feedback parameter λ processing chain. From the post processed timeseries of N and its uncertainties, generates n solutions of N. From n solutions of N, n post-processed solutions of F, and one post-processed time series of T, regress λ n times across time using time windows >= 25 years and compute the λ median across n.

4.4.2.2. Mathematical statement

4.4.2.2.1. Uncertainty propagation

Similarly to the uncertainty propagation of the heat uptake time series in section 4.5.2.2.4., we compute a variance-covariance matrix from the post-processed N time series and its uncertainties to which we can randomly generate n time series of N (as many as F).

4.4.2.2.2. λ regression across sliding windows

A linear regression of ΔN - ΔF on ΔT is repeated at each iteration of a sliding time window of length w. We consider all windows of more than 25 years between 1957 and 2017. In total, between 1957 and 2017, there are 35 successive 25-year windows, 34 successive 26-year windows, etc., and one single 61-year window. For each window, the median of the n values of λ is selected, and a time series of those medians is built for each window length (Figure 7).

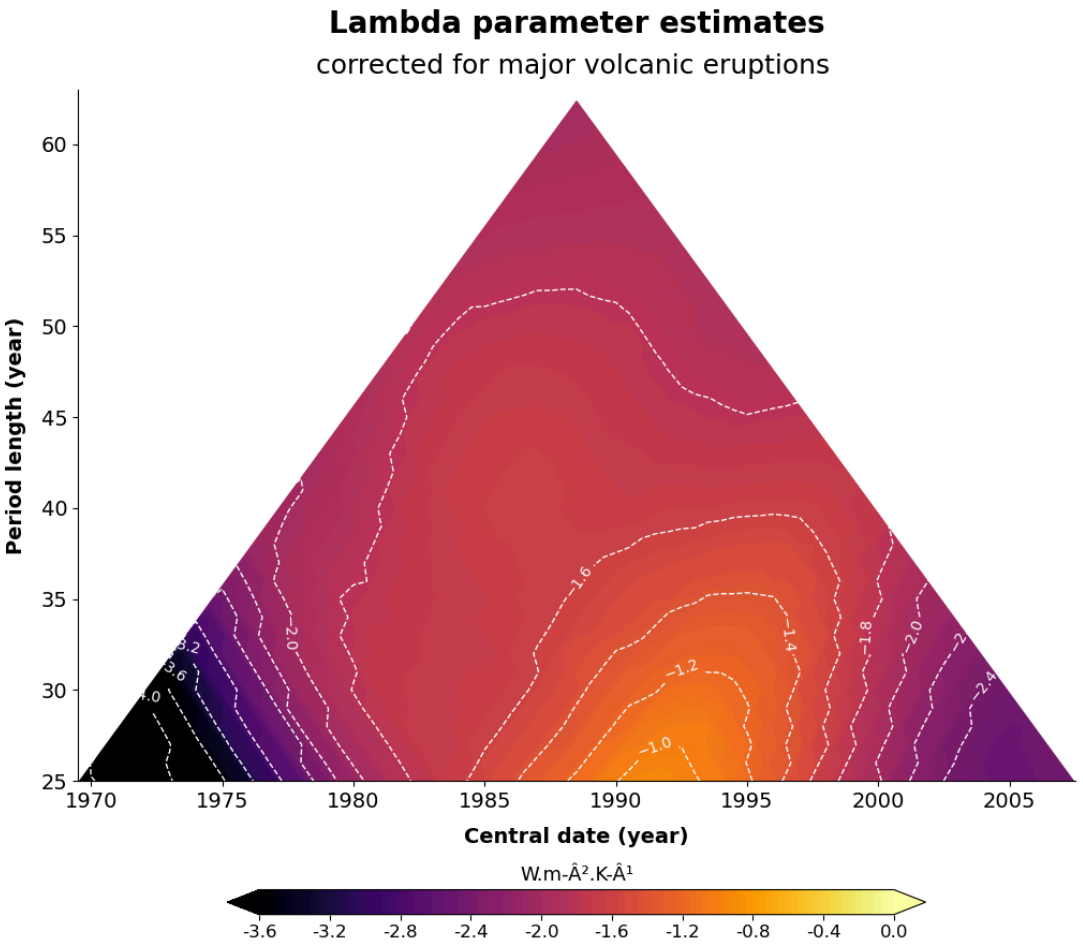

Figure 7. Estimates of the median climate feedback parameter. Climate feedback parameter λ estimated over any window longer than 25 years included within 1957–2017. The vertical axis indicates the length of the window in years. The horizontal axis indicates the central date of the window in years (as an example, the first 25-year window covers the period 1957–1982 and its central date is 1970 thus its coordinates on the triangle are x = 1970, y = 25).